Measurement of Contaminant Concentration Distribution Using Image Processing Techniques

Nobuyuki Kobayashi[a,1], Kazuhide Ito [a], Robert N Meroney [b], Cheng-Hsin Chang [c]

[a]*Tokyo Polytechnic University, Iiyama, Atsugi, Kanagawa, Japan*
[b]*Colorado State University, Fort Collins, CO, USA*
[c]*Tamkang University, Tamsui, Taipei, Taiwan*

ABSTRACT: A new measurement system for wind tunnel tests on environmental dispersion of contaminant concentrations was studied. The concentration measurement system comprised a line scan camera (LSC), an argon ion laser for visualization, an aerosol generator for seeding particles, and a computer for processing the data. This paper reports on the result of the measurement of the averaged concentration and concentration fluctuations of a tracer gas from a point source for two kinds of flow field (channel flow and back step flow) using the system.
There was a linear relationship between concentration and pixel value. It was confirmed that the concentration measurement system can be used for wind tunnel measurements with practical precision after obtaining an accurate calibration curve.

KEYWORDS: Dispersion; Contaminant; Concentration; Concentration fluctuation; Image processing; Line scan camera

1 INTRODUCTION

Various measuring instruments have been used to measure concentrations in wind tunnel tests. However, these concentration measuring instruments have not generally given a high response, although the result of concentration fluctuation measurements with a high-response hydrocarbon analyzer have been reported [1, 2]. Even the high-response hydrocarbon analyzer cannot avoid disturbing the flow field because it must be present itself in the flow. Since concentration is measured at one point in space in these instruments in principle, it is difficult to carry out multipoint concentration measurements at the same time. PIV (Particle Image Velocimetry) has been developed recently and put into practical use. This system can be used as a concentration measurement system by using special components including fluorescence as a tracer gas, and the result of concentration measurements with this system are reported here. However, the PIV system is generally costly, and therefore it is not in widespread use. Against this background, the purpose of this research is to develop a concentration measurement system that has a high response, that can take multipoint measurements, and that is comparatively simple and inexpensive.

2 OUTLINE OF MEASUREMENT SYSTEM

2.1 *System Configuration for Measuring Concentration*

The concentration measurement system comprises a line scan camera (LSC), an argon ion laser with a 4W maximum output for visualization, an aerosol generator for seeding particles, and a computer for data acquisition and processing. An outline flowchart of the system is shown in Fig. 1. Image pixel value B' is measured with a LSC after seeding particles as it passes through the line of the laser, and is stored as image data in the computer. The line scan camera used in

this system has 8-bit resolution. The measurement line corresponding to the line of the laser is resolved into 512 pixels, the background value is deducted, and it is then transformed into concentration information by referring to the calibration curve.

2.2 *Tracer Gas*

DOP (dioctyl phthalate) diluted with ethanol is used to give seed particles with a diameter of about 1μm. Particles are seeded into the flow field from the aerosol generator at a constant rate.

2.3 *Calibration Method and Calibration Curve*

The data stored in the computer is the pixel value corresponding to the luminance value when the particle passes through the laser line. The calibration curve is needed to transform the pixel value into concentration information. A sealed test chamber for the calibration and the experimental arrangement are shown in Fig. 2. A certain amount of tracer gas was injected into the chamber and the pixel value was measured after the gas in the chamber was fully agitated by a fan installed in the upper part of the chamber space. Fig. 3 shows an example of the image data obtained by the LEC. The concentration of the tracer gas C (g/m^3) can be determined from the amount of tracer gas injected and the volume of the chamber V (m^3). The calibration curve is shown in Fig. 4. The tracer gas concentration C was changed in the range of 0 to 0.13 (g/ m^3), and the pixel value B' varied from 0 to 60. It was confirmed that there is almost a linear relationship between the tracer gas concentration and the pixel value. Using a linear approximation, the calibration curve used in this study is as follows:

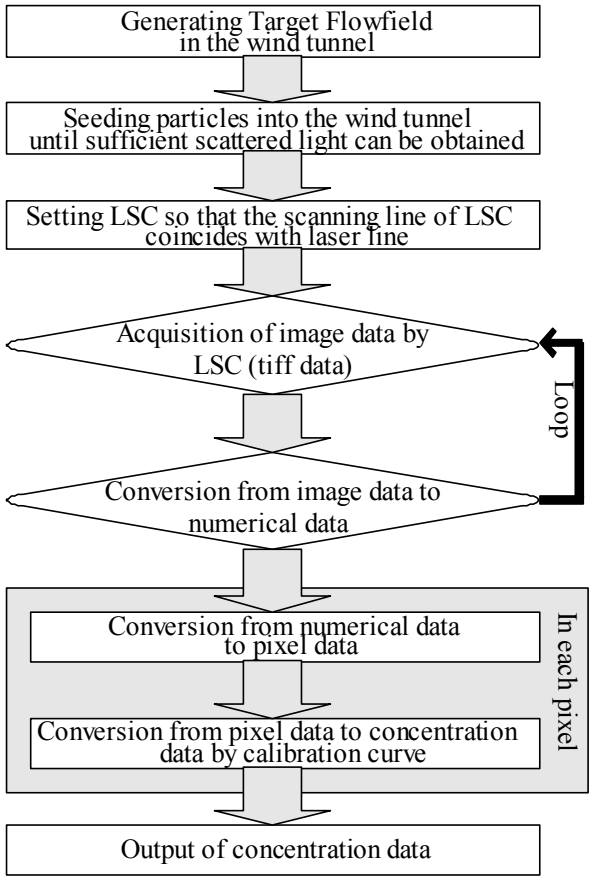

Figure 1 Outline flowchart of the system

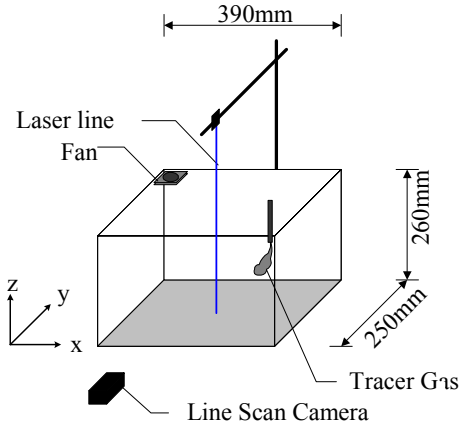

Figure 2 Sealed test chamber for the calibration

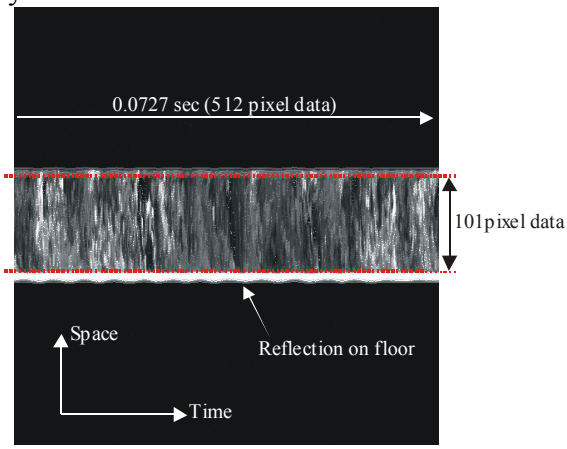

Figure 3 Example of image data

$$C = 2.0E^{-3} \times B'$$

C (= m / V) : concentration of tracer gas
m: emission rate of tracer gas
V: volume of test chamber
B'(= B − B_0): pixel value
B: observed pixel value
B_0: background pixel value

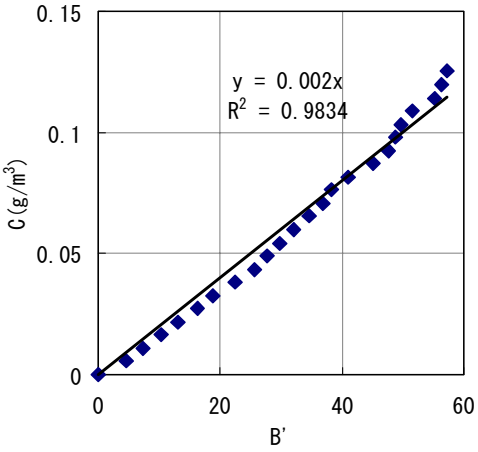

Figure 4 Calibration curve

3 CONCENTRATION MEASUREMENT IN SIMPLE FLOW FIELDS

3.1 *Experimental Setup*

The small wind tunnel shown in Fig. 5 is used for concentration measurements. The size of the tunnel is 2000mm (x) × 300mm (y) × 300mm (z). The wind tunnel is made of acrylic plates. The floor and one of the side walls are painted black to allow the LSC data to be taken clearly. The wind tunnel has a rectifying grid composed of a perforated metal panel of open area ratio 20% and aluminum honeycomb.

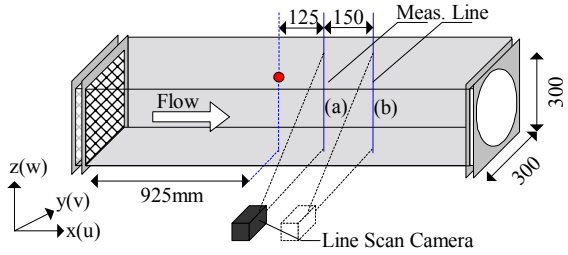

(1) Channel flow

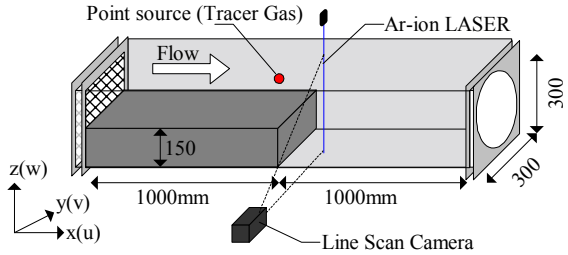

(2) Back step flow

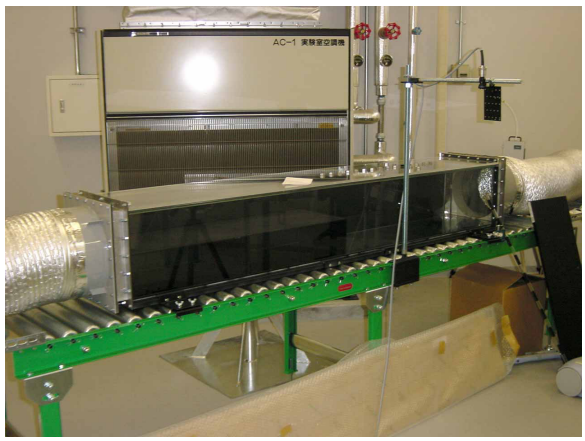

(3) Photo of wind tunnel outline

Figure 5 Small wind tunnel used for the experiments

Averaged concentration and concentration fluctuation in the flow fields are measured using the calibrated concentration measurement system. The contaminant source position and measurement lines are shown in Fig. 6. The origin for the Cartesian coordinate system is located on the most leeward side of an obstacle on the wind tunnel floor. The contaminant point source is located at x=-75mm, y=150mm (center of the wind tunnel width), z=225mm. The contaminant is discharged vertically downward. The diameter of the pipe that discharges the contaminant is 5mm. The emission rate of contaminant is adopted 0.5g/h in consideration of a pixel value to be measured and the extent of the calibrated concentration C (g/m^3). The position of the measurement lines are x=50mm (line A) and x=200mm (line B). The sampling frequency of the concentration measurement is 1 Hz and the sampling duration is 200sec.

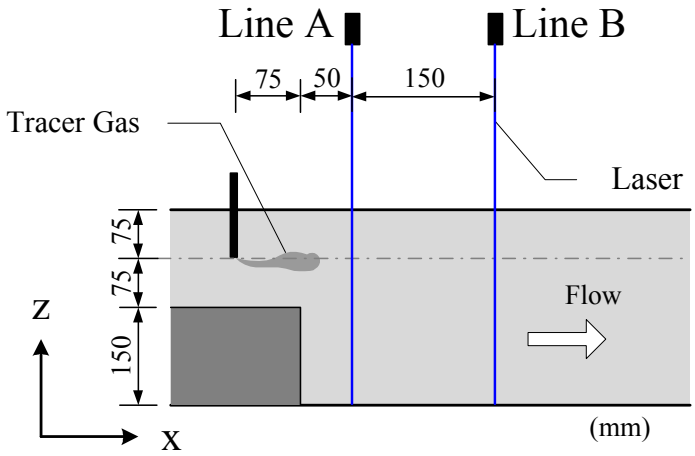

Figure 6 Contaminant source position and measurement lines

4 EXPERIMENTAL RESULTS AND DISCUSSION

4.1 *Velocity and Turbulence Intensity of Approaching Wind*

Vertical profiles of the wind velocity and turbulence intensity at the point x=750mm, y=150mm are shown in Fig. 7. The wind velocity is normalized by the velocity at a height of z=150mm. The dimensionless velocity (u^*) in the channel flow has a convex distribution in which the wind velocity is larger in the central part and becomes smaller as the measurement point approaches the floor and ceiling surface. The turbulence intensity (TI) becomes larger as the point approaches the wind tunnel floor.

In the back step flow, since air flow becomes stagnant in the wake behind the obstacle, u^* becomes gradually smaller in the wake, whereas TI becomes larger. The horizontal profile of the wind velocity at a height of z=150mm is shown in Fig. 8. In the channel flow, u^* has a convex distribution in the central part of the wind tunnel, as for the vertical profile. TI becomes larger as the measurement point approaches the side wall. In the back step flow, u^* in the central part of the wind tunnel (y=150mm, z=150mm) is smaller than near the side wall, and the turbulence intensity TI is larger.

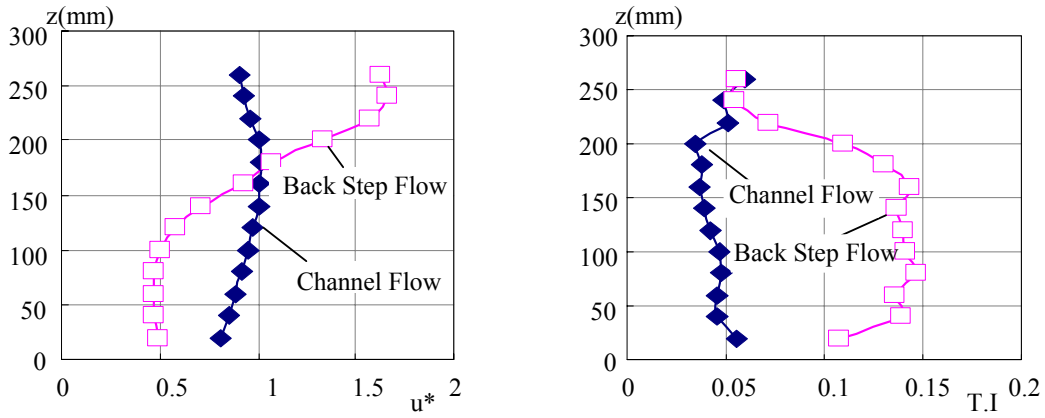

Figure 7 Wind velocity and turbulence intensity (vertical profile)

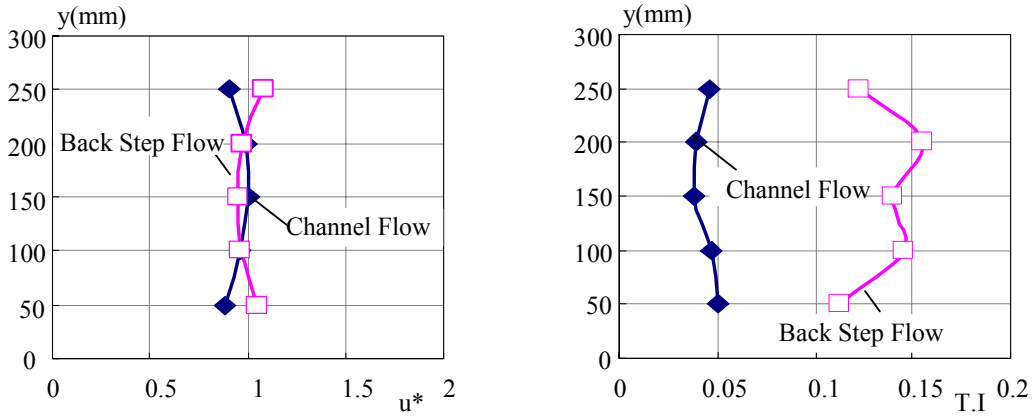

Figure 8 Wind velocity and turbulence intensity (horizontal profile)

4.2 *Averaged Concentration*

For each flow field (channel flow and back step flow), the vertical concentration distributions at measurement lines A and B are measured when contaminant is discharged from the point source at an emission rate of about 0.5g/h. The concentration distribution in the channel flow is shown in Fig. 9 (1), and the distribution in the back step flow is shown in Fig. 9 (2).

All of the concentration distribution curves have a peak and the concentrations descend as their measurement points depart further vertically from the height of the peak point. These concentration distributions correspond to the phenomena actually observed. These distribution curves are considered to provide satisfactory results.

Comparing the maximum value of the concentration on measurement lines A and B, the maximum values in both flow conditions on line A are higher than that on line B, and the peak on line A has also a steeper peak than that on line B, since line A is located nearer to the point source. The height at which the peak appears is lower than the point source height for both flow conditions. This is thought to be because the tracer gas is discharged vertically downward at the source. The peak height is somewhat higher in the back step flow than in the channel flow. This is thought to be due to the fact that since the air flow rates in the wind tunnel in both flow conditions are equal, the wind velocity in the upper part of the obstacle becomes higher in the back step flow than in the channel flow, and the tracer gas flows downstream rapidly in the back step flow before it goes downward.

Since the laser is also reflected at the floor and the ceiling, measurement errors arise near z=0 and 300mm as shown in Fig. 9.

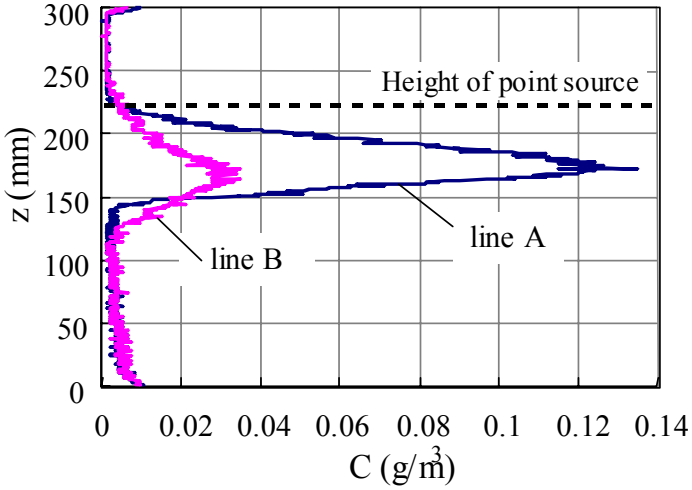

(1) Channel flow

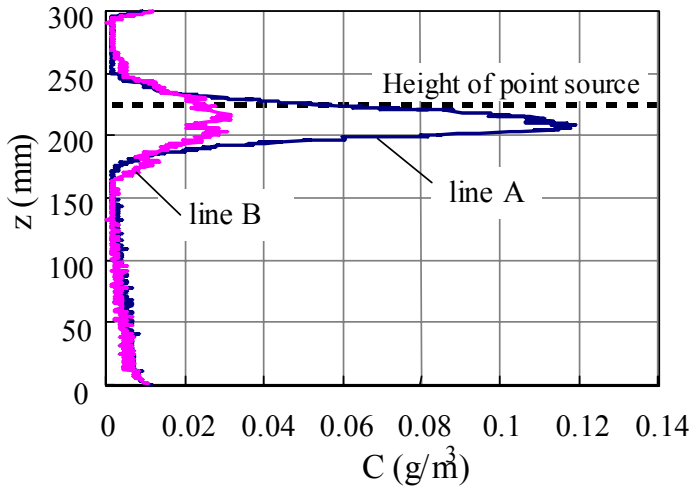

(2) Back step flow

Figure 9 Concentration distribution

4.3 *Concentration Fluctuation*

The time series for the concentration at the point of z=75, 225mm on the line A (x=50mm) in each flow is shown in Fig. 10. The averaged concentration C_{ave} and the standard deviation σ are shown in Table 1. C_{ave} for the channel flow gives a value of 8.0×10^{-4} g/m^3 at both heights. σ is 5.0×10^{-4} g/m^3 at z=75mm, and 2.6×10^{-3} g/m^3 at z=225mm.
C_{ave} for the back step flow gives a value of 10.9×10^{-3} g/m^3 at z=225mm, and C_{ave} at z=75mm gives a value of 7.0×10^{-4} g/m^3. σ is 1.65×10^{-2} g/m^3 at z=225mm, and 5.0×10^{-4} g/m^3 at z=75mm.

The averaged concentrations at a height of z=75, 225mm in the channel flow are very low as shown in Fig. 9, and thus the concentrations could barely be detected as shown in Fig. 10 (1). No concentration could be detected at z=75mm in the back step flow for the same reason. At a

height of z=225mm in the back step flow, concentration fluctuations with intermittent high peaks are observed, which reach the decuple to centuple value of the averaged concentration. This aspect of the concentration fluctuations corresponds to the results of other researchers [3].

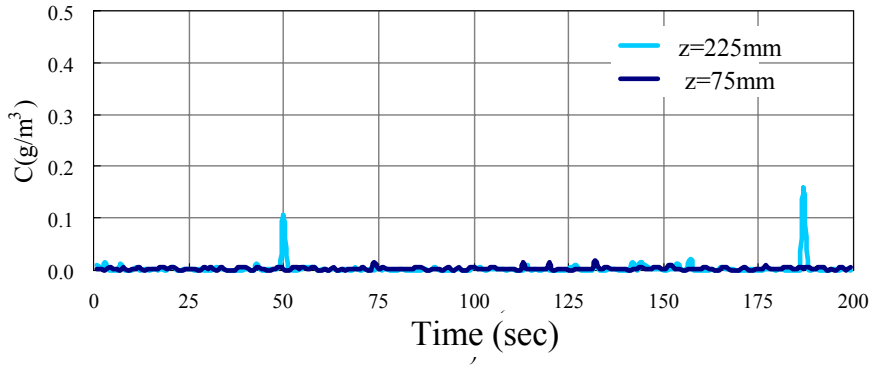

(1) Channel Flow

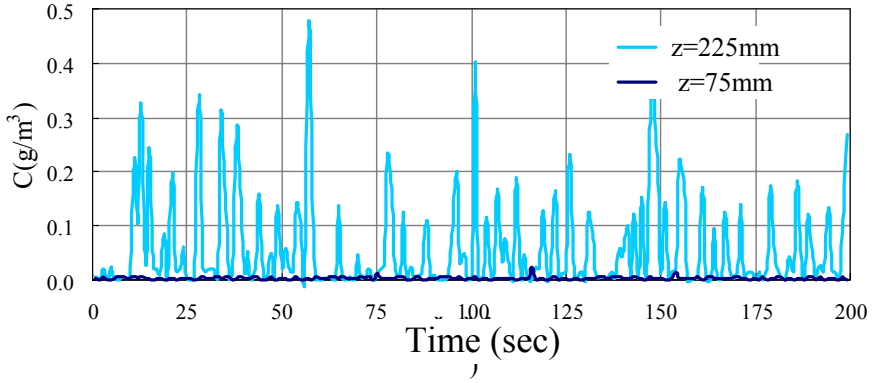

(2) Back Step Flow

Figure 10 Time series for the concentration fluctuations

The characteristics of the averaged concentration distributions and the fluctuations are roughly similar to the results of other researchers and the measurements using this system seem to have detected the concentration correctly. However, a more strict examination of measurement accuracy is needed by comparing the result with those measured by a high response FID system under the same experimental conditions. Furthermore, a calibration method must be developed that is applicable over a wider range of concentration values. Improvements in the computer system to allow higher sampling frequencies are also needed.

5 CONCLUSIONS

A concentration measurement system using a line scan camera was developed for use in dispersion studies. The performance of the system was examined by measuring the averaged concentration and concentration fluctuations in two kinds of flow fields. The results are summarized as follows:

(1) There was a linear relationship between the concentration and the pixel value obtained from the LSC.

(2) The concentration distribution curves reach a peak and the concentrations descend as their measurement points depart further vertically from the height of the peak point. These concentration distributions correspond to the phenomena actually observed. These distribution curves are considered to provide satisfactory results.
(3) After obtaining an accurate calibration curve, it was confirmed that the concentration measurement system can be used for wind tunnel measurements with practical precision.

6 ACKNOWLEDGEMENTS

The authors sincerely acknowledge the financial support from the Ministry of Education, Culture, Sports, Science and Technology of Japan through its Academic Frontier Program for this work. Thanks are extended to the staff of the Wind Engineering Research Center, Tokyo Polytechnic University for their support during the work.

7 REFERENCES

1 Poreh M and Cermak J E. Small-scale Modeling of Line Integrated Concentration Fluctuations. *Proceedings of Sixth U.S. National Conference on Wind Engineering,* Houston, Texas, 1989.3.
2 A Mochida, S Murakami, T Takahashi et al. Experimental Study on Gas Concentration near Building Using High Frequency Response FID. Journal of Japan Association for Wind Engineering, pp. 55-56, 2001.10.
3 Y Tominaga, S Murakami, A Mochida et al. Wind Tunnel Tests on Turbulent Diffusion and Concentration Fluctuation of Buoyant Gas near Buildings. *Proceedings of the Twelfth Wind Engineering Symposium in Japan*, 1992.12.
4 Cheung J C K and Melbourne W H. Spectral Properties of Dispersion from a Model Plume in Turbulent Wind Flows. *Proceeding of The Fifth Asia-Pacific Conference on Wind Engineering, Kyoto, Japan,* pp. 301-304, Special Edition of Journal of Japan Association for Wind Engineering, 2001.10.